

# THE USE OF GLOBAL SENSITIVITY ANALYSIS FOR ASSESSING CAPABILITY OF THE MTG/FCI INSTRUMENT TO DETECT AEROSOLS

Youva Aoun, Philippe Blanc, Lucien Wald, Sandrine Mathieu, Marine  
Claeyman

► **To cite this version:**

Youva Aoun, Philippe Blanc, Lucien Wald, Sandrine Mathieu, Marine Claeyman. THE USE OF GLOBAL SENSITIVITY ANALYSIS FOR ASSESSING CAPABILITY OF THE MTG/FCI INSTRUMENT TO DETECT AEROSOLS. 2015 EUMETSAT Meteorological Satellite Conference, EUMETSAT, Sep 2015, Toulouse, France. Aoun.pdf. hal-01290979

**HAL Id: hal-01290979**

**<https://hal-mines-paristech.archives-ouvertes.fr/hal-01290979>**

Submitted on 19 Mar 2016

**HAL** is a multi-disciplinary open access archive for the deposit and dissemination of scientific research documents, whether they are published or not. The documents may come from teaching and research institutions in France or abroad, or from public or private research centers.

L'archive ouverte pluridisciplinaire **HAL**, est destinée au dépôt et à la diffusion de documents scientifiques de niveau recherche, publiés ou non, émanant des établissements d'enseignement et de recherche français ou étrangers, des laboratoires publics ou privés.

## THE USE OF GLOBAL SENSITIVITY ANALYSIS FOR ASSESSING CAPABILITY OF THE MTG/FCI INSTRUMENT TO DETECT AEROSOLS

Youva Aoun<sup>1</sup>, Philippe Blanc<sup>1</sup>, Lucien Wald<sup>1</sup>, Sandrine Mathieu<sup>2</sup>, Marine Claeys<sup>2</sup>

<sup>1</sup>MINES ParisTech, PSL Research University, O.I.E. – Centre Observation, Impacts, Energy, CS  
10207 rue Claude Daunesse 06904 Sophia Antipolis Cedex, France

<sup>2</sup>Thales Alenia Space, 5 allée des Gabians, BP 99, 06156 Cannes La Bocca Cedex, France your

**The Flexible Combined Imager (FCI) is an instrument to be borne by the future geostationary meteorological satellite Meteosat Third Generation (MTG). A numerical simulator was set up to provide simulated outputs of the instrument. It includes top-of-atmosphere scene of upwelling spectral radiance obtained by a radiative transfer model in the clear atmosphere, and the transfer function of the FCI. The sensitivity of the sensor outputs to aerosol properties is studied by varying the inputs defining the scenes and their illumination. The Global Sensitivity Analysis (GSA) with the Sobol' decomposition is applied to the outputs of the simulator, yielding a ranking of the inputs with respect to their influence on the FCI numerical outputs. The results are presented for all visible and near infrared channels of the FCI for desert type of aerosols according to the OPAC database. The study highlights the most relevant channels for aerosol detection and characterization and gives assessment of the different sources of uncertainties in aerosol retrieval with such channels.**

### INTRODUCTION

This communication aims at investigating benefits of the Global Sensitivity Analysis (GSA) to assess the capabilities of future space borne radiometers. This study is conducted on the Flexible Combined Imager (FCI) as the main payload of the future geostationary meteorological satellite Meteosat Third Generation (MTG). Meteorology, air pollution monitoring, air plane security or solar energy conversion might benefit from the FCI characteristics in term of spatial, temporal and spectral resolutions.

A simulator of the signal output by the instrument has been built to assess the capability of the FCI to characterise properties of aerosols such as their concentrations and their types. The simulator includes the computation of the upwelling spectral radiance at the top of atmosphere (TOA) originating from a scene at ground level obtained by a radiative transfer model in cloud free atmosphere, and the transfer function of the FCI (spectral response, radiometric noise, etc.) to yield the signal output by the instrument.

Sensitivity analysis is commonly used in remote sensing (Aminou et al. 1999; Prigen et al. 2001). Morris method, local sensitivity analysis or one factor at a time (OAT) suffer drawbacks such as calculation time, failure to estimate the coupling between inputs or restricted range of variation of inputs. The use of the global sensitivity analysis (GSA) addresses several of these issues. It requires realistic randomly drawn set of atmospheric state. This communication shortly introduces the FCI instrument and its specifications used for the simulations. Then it presents the models and data used as input to the simulator, and to generate set of realistic atmospheric state. Then, the main principles and equations related to the use of the GSA are introduced. Finally the results of the GSA are discussed for a case study of desert dust over a desert ground.

### CASE STUDY MTG/FCI

As the prime contractor of the MTG mission, Thales Alenia Space (TAS) is interested to know the future capability of the FCI in observing the aerosols and has co-funded a PhD thesis to assess this point. This paper presents part of this work. The MTG will embed two different missions. The Imager MTG-I mission, encompassing two instruments, the FCI (Flexible Combined Imager) and the LI (Lighting Imager). FCI has a strong heritage of the current MSG SEVIRI payload series and will provide complete scan every 10 min with a nadir spatial resolution of 1 km and 500 m for visible channels and 1 km and 2 km for thermal channels. The Sounder MTG-S mission, with IRS

interferometer and UVN, an UV spectrometer, will give 3D views of the atmospheric layers. MTG will orbit at an altitude of about 36000 km over the Gulf of Guinea at the 0° latitude and will be 3-axis stabilized. The development and procurement of MTG-I is under the responsibility of ESA. TAS leads an industrial consortium of more than 50 European companies which develop, manufacture, integrate and test the spacecraft. The main payload, the FCI, is developed by TAS France.

The FCI acquires images in the 16 channels represented in the Table 1. Eight of these channels are placed in the solar spectral domain between 0.4  $\mu\text{m}$  to 2.1  $\mu\text{m}$ . The other eight channels are in the thermal spectral domain between 3.8  $\mu\text{m}$  to 13.3  $\mu\text{m}$ . This study is focused on the eight visible and near infrared channels (VNIR) of the FCI for which optical properties and behavior of dust aerosols can be retrieved from *in situ* measurement network.

| Channel                    | Central wavelength, $\lambda_0$ ( $\mu\text{m}$ ) | Bandwidth, $\Delta\lambda_0$ ( $\mu\text{m}$ ) | Spatial resolution (km) |
|----------------------------|---------------------------------------------------|------------------------------------------------|-------------------------|
| VIS 0.4                    | 0.444                                             | 0.060                                          | 1.0                     |
| VIS 0.5                    | 0.510                                             | 0.040                                          | 1.0                     |
| VIS 0.6                    | 0.640                                             | 0.050                                          | 1.0; 0.5                |
| VIS 0.8                    | 0.865                                             | 0.040                                          | 1.0                     |
| VIS 0.9                    | 0.914                                             | 0.020                                          | 1.0                     |
| NIR 1.3                    | 1.380                                             | 0.030                                          | 1.0                     |
| NIR 1.6                    | 1.610                                             | 0.050                                          | 1.0                     |
| NIR 2.2                    | 2.250                                             | 0.050                                          | 1.0; 0.5                |
| IR 3.8 (TIR)               | 3.800                                             | 0.400                                          | 2.0; 1.0                |
| WV 6.3                     | 6.300                                             | 1.000                                          | 2.0                     |
| WV 7.3                     | 7.350                                             | 0.500                                          | 2.0                     |
| IR 8.7 (TIR)               | 8.700                                             | 0.400                                          | 2.0                     |
| IR 9.7 (O <sub>3</sub> )   | 9.660                                             | 0.300                                          | 2.0                     |
| IR 10.5 (TIR)              | 10.500                                            | 0.700                                          | 2.0; 1.0                |
| IR 12.3 (TIR)              | 12.300                                            | 0.500                                          | 2.0                     |
| IR 13.3 (CO <sub>2</sub> ) | 13.300                                            | 0.600                                          | 2.0                     |

**Table 1: Channels of the FCI**

## METHOD

### Simulator definition

Since real images from the FCI are not yet available, a simulator of this instrument was set up using libRadtran, a radiative transfer code library (Mayer & Kylling, 2005). This simulator takes into account several parameters such as TOA solar spectral radiance, atmospheric composition, ground albedo, type and distribution of the aerosols in the atmosphere. For this study, we have selected the Air Force Geophysical Laboratory Mid-latitude Summer (AFGL-MS) (Anderson et al. 1986) as the typical atmospheric profile. Aerosols simulation parameters are the desert type aerosols according to the OPAC database (Hess et al. 1998) included in libRadtran. The simulator output is the reflectance at the TOA observed by the instrument, noted  $\alpha$  and abbreviated in reflectance hereafter. It is defined in the system requirement document (EUMETSAT 2013) as:

$$\alpha = \rho * \cos(\theta_s) \quad (1)$$

where  $\rho$  is calculated using this equation:

$$\rho = \frac{\pi L_\lambda}{E_\lambda^S * \cos(\theta_s)} \quad (2)$$

with  $L_\lambda$  the radiance observed in the channel defined by the central wavelength  $\lambda$ ,  $E_\lambda^S$  the integrated solar spectrum corresponding to this channel and  $\theta_s$  the solar zenith angle. It comes:

$$\alpha = \frac{\pi L_\lambda}{E_\lambda^S} \quad (3)$$

, The ranges of measurements defining the minimal, maximal and reference reflectances that can be observed for each VNIR channel of FCI are given in the Table 2. This table was used in the simulation to exclude cases for which simulated outputs do not meet the radiometric min-max requirement of the instrument.

| Channel | Min. Signal, $\alpha_{min}$ | Max. Signal, $\alpha_{max}$ | Ref. Signal, $\alpha_{ref}$ |
|---------|-----------------------------|-----------------------------|-----------------------------|
| VIS 0.4 | 0.01                        | 1.20                        | 0.01                        |
| VIS 0.5 | 0.01                        | 1.20                        | 0.01                        |
| VIS 0.6 | 0.01                        | 1.20                        | 0.01                        |
| VIS 0.8 | 0.01                        | 1.20                        | 0.01                        |
| VIS 0.9 | 0.01                        | 0.80                        | 0.01                        |
| NIR 1.3 | 0.01                        | 0.80                        | 0.01                        |
| NIR 1.6 | 0.01                        | 1.20                        | 0.01                        |
| NIR 2.2 | 0.01                        | 1.20                        | 0.01                        |

**Table 2: Radiometric requirements of the FCI Images for the VNIR channel**

The retrieval of aerosols, whether *in situ* or remotely, is nowadays almost exclusively conducted for cloud free conditions. Hence, only such conditions are simulated. The sensitivity analysis is conducted on the following inputs:  $\theta_s$ , the ground albedo ( $\rho_g$ ), the aerosols optical thickness ( $\tau$ ), the total column contents of water vapor ( $WV$ ) and ozone ( $O_3$ ). These variables are the main responsible of the variability of the signal in a cloud-free condition. The viewing angles and the solar azimuth angle are equally important but were ignored because the variation associated to them is mainly geometrical and will influence the signal similarly to  $\theta_s$ . The measured reflectance in each channel was computed using the radiometric and spectral specifications of FCI. The simulator has been validated by simulating the outputs for the two visible channels of the MSG/SEVIRI using AERONET level 2.0 data for several measuring sites and comparing these outputs against corresponding actual data from MSG/SEVIRI. The correlation between the simulated outputs the satellites measurements are equal to 0.967 for desert station such as El Farafra and 0.964 for Tamanarasset.

#### Data used

The simulations are performed for realistic atmospheric state. Sensitivity analysis requires large amount of realistic simulations with realistic input parameters. To do so, cumulative distribution functions (CDF) were calculated for each input from *in situ* measurement (AERONET), remote sensing data (MODIS) and reanalysis product (MACC-IFS-NRT). More precisely, the aerosol optical thickness at several wavelengths and total column content of water vapour were retrieved from the level 2.0 data of the AERONET station of Tamanarasset\_INM, in South Algeria. The total column content of ozone was retrieved from the reanalysis product of the MACC project. The MACC project (Monitoring Atmosphere Composition and Climate), funded by the European Commission, is preparing the operational provision of global aerosol property forecasts together with physically consistent total column content in water vapour and ozone (Kaiser et al., 2012a;Peuch et al., 2009). The ground albedo was retrieved from the MODIS combined collection MCD43B3. This albedo product is provided as a 1-km data describing both directional hemispherical reflectance (black-sky albedo) at local solar noon and bihemispherical reflectance (white-sky albedo) at 10 wavelengths (0.47  $\mu\text{m}$ , 0.55  $\mu\text{m}$ , 0.67  $\mu\text{m}$ , 0.86  $\mu\text{m}$ , 1.24  $\mu\text{m}$ , 2.1  $\mu\text{m}$ , 0.3-0.7  $\mu\text{m}$ , 0.3-5.0  $\mu\text{m}$ , and 0.7-5.0  $\mu\text{m}$ ). This ensures that the ground albedo input to the simulator includes the spectral dependency of a realistic albedo. Data from MACC and MODIS were retrieved for Tamanarasset in order to correspond to the measurements of the AERONET station. Each of these atmospheric state inputs to the simulator were then randomly and independently drawn from the CDFs to mimic there observed probability density functions.

#### THE GLOBAL SENSITIVITY ANALYSIS

Inputs to the simulator have their own independent and realistic variability and each one has an impact on the reflectance. Sensitivity analysis can be performed in order to assess the capability of the FCI in observing aerosol properties. There are several methods to perform such sensitivity analysis and the choice of one or another depends on the objectives of the analysis itself and the available means to perform it. The “*One factor At a Time*” (OAT) methods is suitable to evaluate the sensitivity of an instrument to each relevant variable that influences the measure. The Taylor development focuses on the analysis around a critical point of interest. The screening methods offer a sensitivity analysis for a set of random discrete values of inputs. These methods suffer drawbacks. A screening method with too large steps of sampling may miss information. OAT methods fail to estimate the coupling effects between variables. The Taylor development is focused on a limited range of variation of the inputs and variation away of the focus point can stay unnoticed.

The global sensitivity analysis (GSA) is another method used to calculate the influence of inputs to a model. The GSA assesses the sensitivity of a model or an instrument to all relevant inputs on their whole realistic ranges of variations. The GSA is also used to calculate the importance of inputs to models, in order to freeze unimportant inputs and reduce the computational time of model with a large number of inputs (Sobol' et al. 2007). The GSA is used to assess the sensitivity of the FCI to changes in atmospheric state and to deduce that part of the signal variability due to aerosols properties and to the other exogenous variables. The simulator is based on several models and cannot be approximated accurately by an analytical function of every input. Therefore, the sensitivity analysis is performed by analyzing the variance of the simulator outputs randomly drawn as previously described. Let us take a function  $F$  with  $p$  input  $(X_1, X_2, X_3, \dots, X_p)$  and output  $Y$  :

$$\begin{array}{ccc} \mathbb{R}^p & \rightarrow & \mathbb{R} \\ (X_1, X_2, X_3, \dots, X_p) & \mapsto & Y = F(X_1, X_2, X_3, \dots, X_p) \end{array} \quad (4)$$

Here,  $F$  can be viewed as the simulator unknown function and  $Y$  the output of the simulator as the measured reflectance. The GSA is based on the independency hypothesis of the input parameter and on the ANOVA decomposition of  $F$  as a sum of orthogonal functions of increasing number of input parameters:

$$Y = F(X_1, X_2, X_3, \dots) = f_0 + \sum_{i=1}^p f_i(X_i) + \sum_{1 \leq i < j \leq p} f_{ij}(X_i, X_j) + \dots \quad (5)$$

with

$$f_0 = E(Y) \quad (6)$$

$$f_i(X_i) = E(Y | X_i) - E(Y) \quad (7)$$

$$f_{ij}(X_i, X_j) = E(Y | X_i, X_j) - E(Y | X_i) - E(Y | X_j) + E(Y) \quad (8)$$

etc.

The functions  $f_i(X_i)$  is a 1-dimensional function calculated on the range of variation of the  $i^{\text{th}}$  input  $X_i$ . The function  $f_{ij}(X_i, X_j)$  represents the coupling between the  $i^{\text{th}}$  and  $j^{\text{th}}$  inputs  $X_i$  and  $X_j$ .

ANOVA decomposition was introduced in statistical mathematic by (Hoeffding 1948). The use of the ANOVA based method is widely encountered in sensitivity analysis. This decomposition is also known as the Sobol' decomposition (Sobol' 1993). The principle of the Sobol' decomposition is to consider the variance of the reflectance as the sum of the variance due to each inputs taken one by one for the first order, two by two for the second order, etc. It yields that the variance of the output can also be expanded in a sum of increasing dimension calculated from the functional.

$$V(Y) = \sum_{i=1}^p V_i + \sum_{1 \leq i < j \leq p} V_{ij} + \dots \quad (9)$$

with

$$V_i = V(E(Y | X_i)) \quad (10)$$

$$V_{ij} = V(E(Y | X_i, X_j)) - V_i - V_j \quad (11)$$

etc.

The ratio between total variance and the variance due to one input is called the Sobol' index. 1<sup>st</sup> order Sobol' indices are defined as a ratio between variance due to one input ( $V_i$ ) and the total variance of the model ( $V(Y)$ ).

$$S_i = \frac{V_i}{V(Y)} \quad (12)$$

$$S_{ij} = \frac{V_{ij}}{V(Y)} \quad (13)$$

The Sobol' indices reflect the impact of the input variables on the reflectance. Sobol' indices outline the sensitivity of the model to the inputs. The greater a Sobol' index is, the greater is the impact of the corresponding variable on the reflectance.

The Sobol' indices of order 1 to 2 are presented in the Figure 1 for the channel VIS0.4 of the FCI. The first Sobol' index is associated with  $\theta_s$  and is greater than 0.9: the signal variability is highly dominated by the variability of  $\theta_s$ . The second Sobol' index is associated with  $\rho_G$ , the ground albedo, and is significantly less than the first one.

In the case of a retrieval algorithm targeted on other variables such as aerosols, these two inputs would be the main source of exogenous noise. The correlation between  $\theta_s$  and aerosol optical thickness is also an important input as it is the third term ( $\tau, \theta_s$ ). It might stay unnoticed because of the high importance of  $\theta_s$ . The physical meaning of this term and of its importance is currently under assessment.

The Sobol' index associated with  $\tau$  is in fifth position and can be considered as not significant regarding the importance of the previous variables.

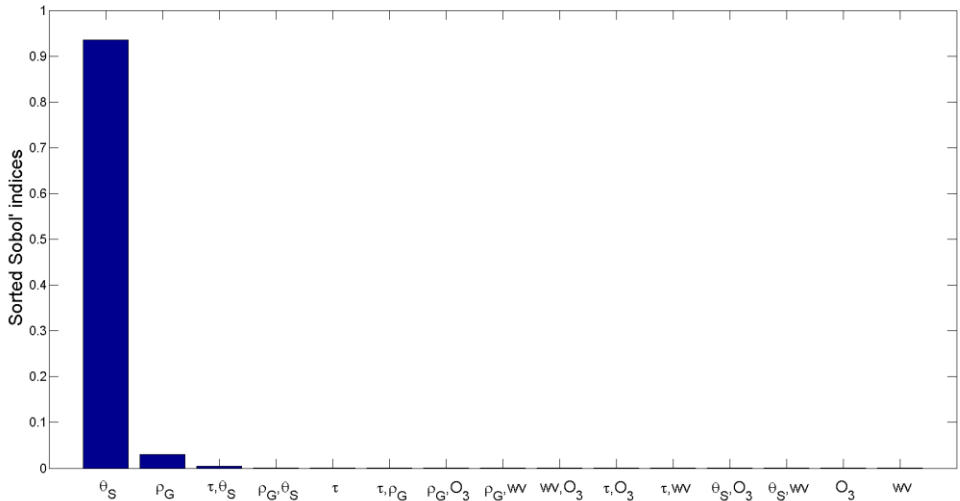


Figure 1: Sobol' indices of order 1 to 2 for the channel VIS0.4 of the FCI

The signal variability is dominated by  $\theta_S$ . The inputs situated from the fourth position to the end have a neglecting influence on the overall signal variability. This underlines the importance of estimating the sensitivity of an instrument also on the possible correlation between variables.

The Sobol' indices are estimated for the channels of the VNIR of the FCI. This type of analysis gives insight on the most relevant channels to be used in aerosols detection. It also gives information on which variables are the principal sources of noise on the signal regarding the variable of interest. It gives information on the level of knowledge of other inputs needed to perform the retrieval.

RESULTS AND DISCUSSION

We present the result for the VNIR channel of the FCI and one OPAC type of aerosols: desert type (Hess et al. 1998). The ground albedo that is considered here corresponds to the desert ground of Tamanrasset. This corresponds to a typical environment for desert dust that is emitted and transported.

In order to present the result for the 8 VNIR channels of FCI, the Sobol' indices have been stacked on bar. Each bar represents the Sobol' indices calculated for one channel as presented in the Figure 1. In the Figure 2 the aerosol optical thickness ( $\tau$ ) is represented in pink in order to be discriminated from surrounding colours. There is no visible pink rectangle for the channels presented here:  $\tau$  represents no significant part of the variability of the signal in any channel of the VNIR, in a varying realistic atmospheric state over a desert ground.

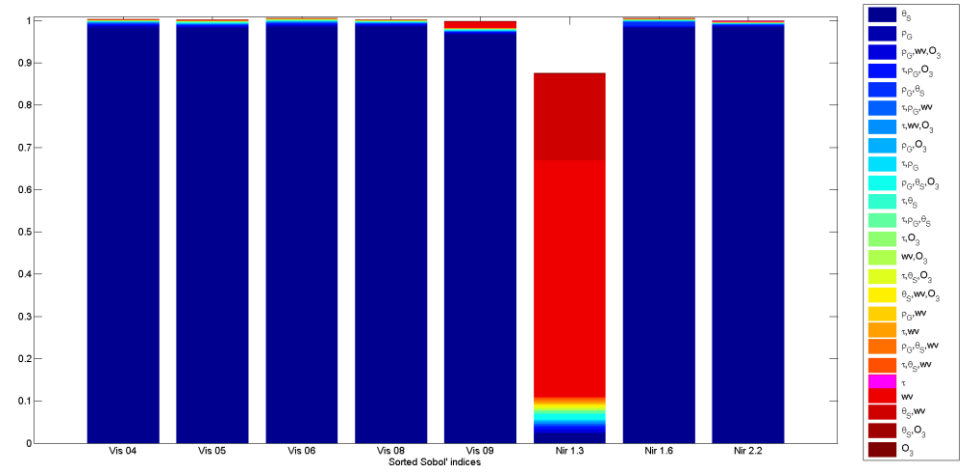


Figure 2: Sobol' index of order 1 to 3 for the channel of the VNIR of the FCI

In this figure, the bar representing the channel NIR 1.3 show a very different behaviour compared to others. As said before, the simulations were made for cloud free condition. The NIR 1.3 channel was

designed namely to observe cirrus and clouds in the upper atmosphere. The simulator takes into account the dynamics of the FCI channels as they were defined in the system requirement document and represented in the Table 2.: A majority of the simulated measurements in this channel were rejected as the signal was not significant enough to be measured. Therefore only 20 % of the 200 000 simulated measures were used for the sensitivity analysis for this channel. Moreover, an absorbing band of the water is present in the part of the solar spectrum observed by this channel. The weighting function of the channel leads to a poor capacity to observe the lower part of the atmosphere. As the desert aerosols are mostly contained in the boundary layer and the troposphere, the channel is obviously not suitable to observe aerosols.

In the Figure 2,  $\theta_s$ , the ground albedo and their coupling are the most important inputs of the simulator. This demonstrates the good agreement of the simulator output with the physics behind the radiative transfer equation. The solar illumination conditions and the ground albedo have a major impact on the quantity of light observed by a space borne imager. The part of the signal variability due to aerosols is masked and can be considered as not significant due to the large influence of  $\theta_s$ .

Nevertheless,  $\theta_s$  is known with high precision from geometrical calculation. As shown in the equation (5), the GSA methodology considers the reflectance  $\alpha$ , as a function of several variables and decomposes it as a sum of functional:

$$\alpha = f(\theta_s) + G(\tau, \rho_G, \dots) \quad (14)$$

Using equation (14) the influence of  $\theta_s$  can be subtracted as follows:

$$\alpha' = \alpha - f(\theta_s) = G(\tau, \rho_G, \theta_s \dots) \quad (15)$$

This operation can be applied not only for the direct influence of  $\theta_s$  but also for the influence of the ground albedo as it can be estimated from other satellites data or jointly estimated with  $\tau$  (Carrer et al. 2010). The residual reflectance  $\alpha'$  can be then used to apply another GSA in order to determine the influence of the remaining inputs plus the one we subtracted. As the ANOVA functions are only estimated, they cannot completely and perfectly represent the influence of the exogenous variables and therefore completely remove their influence.

The results of the GSA conducted on the residual reflectances are presented in the Figure 3.  $\tau$  is highlighted in pink and can be discriminated from the other inputs on almost all channels of the VNIR of the FCI. The influence of  $\tau$  was revealed by the subtraction of the influence of exogenous variables. The part of the signal variability due to the variation of the quantity of aerosols is different for every channel and shows a spectral dependency, as expected.

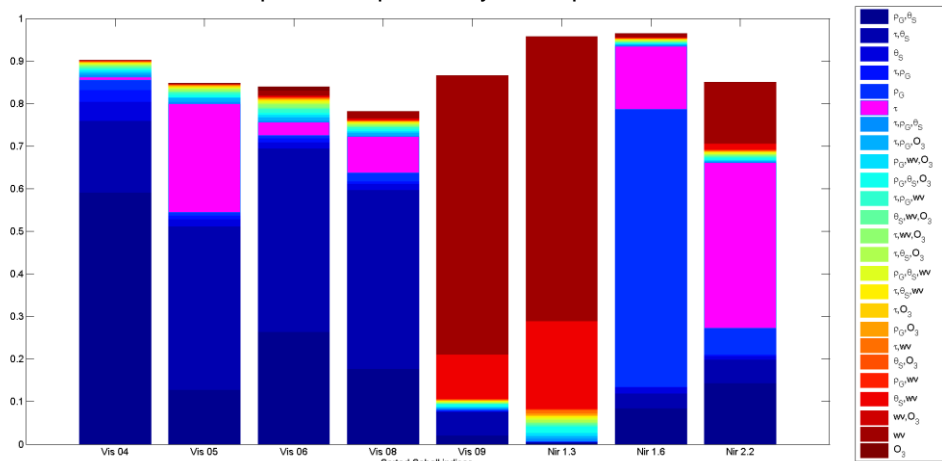


Figure 3: Sobol' index of order 1 to 3 for the channel of the VNIR of the FCI

The channel VIS0.9 displays a behavior which seems to be similar to the NIR1.3. Another absorption band of the water is indeed located in the part of the solar spectrum measured by this channel. This behavior was masked by the influence of  $\theta_s$  and  $\rho_G$  in the first GSA. By subtracting their influences, unnoticed information was highlighted which is one of the benefit of the Sobol' decomposition.

In the Figure 3, the channel VIS0.4 shows a weak sensitivity to the variation of  $\tau$ . The signal variability is mostly dominated by the coupled term ( $\rho_G, \theta_s$ ). This result requires further investigation especially if one wants to remove this term.

The VIS0.5 and VIS0.6 channels show different responses to the variability of aerosols. These differences can be associated with the physical properties of the aerosols such as the single scattering albedo (SSA) shown in the Figure 4. For the part of the spectrum corresponding to the channel VIS0.5

the SSA is around 0.83 denoting the absorption of a significant part of the solar radiation. Whereas the SSA corresponding to the channel VIS0.6 is greater than 0.91 denoting a lower quantity of solar radiation absorbed by atmospheric aerosols and the influence of  $\tau$  on the signal is reduced accordingly.

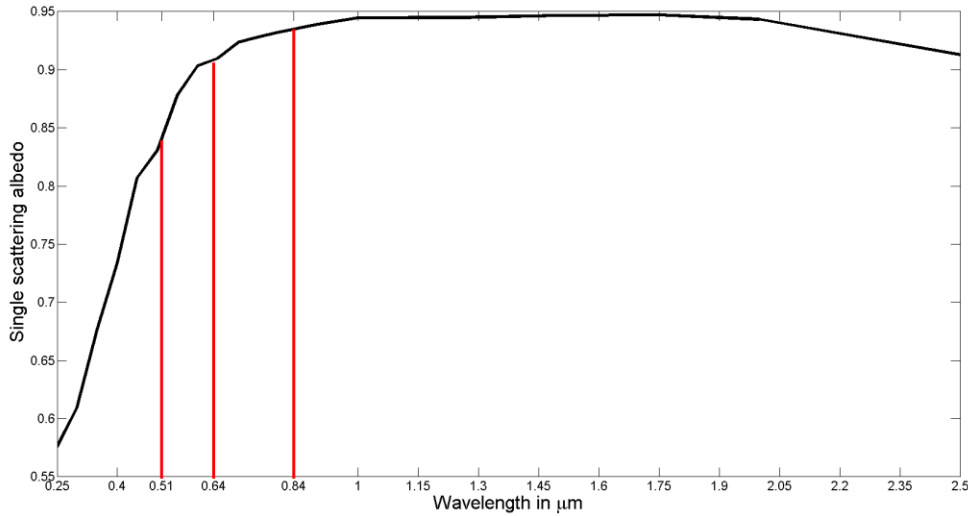


**Figure 4:** Single scattering albedo of mineral dust in the visible and near infrared according to OPAC. The 3 red lines represent the central wavelength of the channels VIS0.5, VIS0.6 and VIS0.8 of the FCI.

The VIS0.6 and VIS0.8 channels show also significant differences regarding the part of the signal variability due to aerosols. The dynamics of the signal measured in these channels may explain these discrepancies. The total variance of the signal is given in the Table 3 for each channel. The variance of the signal of the channel VIS0.8 is greater than that of the channel VIS0.6. This can explain the discrepancy but further analysis must be performed to offer a more satisfactory and solid explanation.

| Channel                     | VIS04  | VIS05  | VIS06  | VIS08  | VIS09  | NIR1.3 | NIR1.6 | NIR2.2 |
|-----------------------------|--------|--------|--------|--------|--------|--------|--------|--------|
| Variance of the reflectance | 0.0177 | 0.0198 | 0.0485 | 0.0691 | 0.0495 | 0.0015 | 0.1009 | 0.0948 |

**Table 3:** Dynamics of the channels of the visible and near infrared part of the spectrum of the FCI.

Both the NIR1.6 and NIR2.2 channels exhibit a significant part of the signal influenced by the aerosols. Future retrieval algorithms should take into account the result of this type of analysis to assess the uncertainties associated to the retrieval the aerosol optical properties with this instrument for this channel and in these conditions. According to these results, several VNIR channels of the FCI might be suitable for the retrieval of the aerosols optical properties. Nonetheless exogenous sources of variability such as  $\theta_s$  and  $\rho_G$  have been identified by the GSA methodology and should be known prior to the retrieval to reduce the uncertainty.

## CONCLUSIONS

It has been shown that the global sensitivity analysis can be useful for assessing the capability of future space borne instrument. The methodology highlights the importance of coupling between some of the inputs. The ANOVA decomposition used here leads to the unveiling of the uncertainty due to known variables such as the solar zenith angle or the ground albedo. The GSA offers access to the estimation of the part of the signal variability due to aerosol optical thickness and therefore their observability in the different channels of the instrument for the visible and near infrared.

These calculations were done for a simple, ideal case with a reduced number of inputs. The methodology has proven to be of interest and provides interesting and consistent information. These results show a variable sensitivity of the FCI to the variation of aerosols properties in the realistically varying atmospheric state for several channels of the instrument in the VNIR part of the spectrum. Other not shown calculations were made in a case of an observation of dust aerosols over sea and show significantly better results in term of observability of aerosol properties. Other simulations will be conducted with more inputs, including the angle of view or the description of microphysical properties of desert aerosols.



## ACKNOWLEDGEMENT

The authors thank Emilio Cuevas-Agullo and his staff for their effort in establishing and maintaining Tamanrasset\_INM site. Youva Aoun is currently performing a PhD Thesis at MINES ParisTech funded by Thales Alenia Space and Conseil Régional de Provence-Alpes-Côte-d'Azur. The authors acknowledge that the MTG satellites are being developed under an ESA contract to TAS-F and thank Region PACA for its financial support.

## REFERENCES

- Aminou, D. M. A., Ottenbacher, A., Jacquet, B., Kassighian, A. (1999) Meteosat second generation: on-ground calibration, characterization, and sensitivity analysis of the SEVIRI imaging radiometer. In Proc. SPIE 3750, Earth Observing Systems IV (24 September 1999), 419-430
- Anderson, G. P., Clough, S. A., Kneizys, F. X., Chetwynd, J. H., Shettle, E. P. (1986) AFGL Atmospheric Constituent Profiles (0.120 km). Tech. report, AFGL-TR-86-0110, Air Force Geophysics Lab., Hanscom Air Force Base, MA, USA, 43 pp
- Carrer, D., Roujean, J.-L., Hautecoeur, O., Elias, T. (2010) Daily estimates of aerosol optical thickness over land surface based on a directional and temporal analysis of SEVIRI MSG visible observations. *J. Geophys. Res.*, **115**, D10208
- EUMETSAT (2013) MTG System Requirements Document (SRD). Retrieved April 18, 2014, from <http://www.eumetsat.int/website/home/Satellites/FutureSatellites/MeteosatThirdGeneration/MTGResources/index.html>
- Hess, M., Koepke, P., Schult, I. (1998) Optical properties of aerosols and clouds: The software package OPAC. *Bull. Amer. Meteor. Soc.*, **79**, pp 831–844
- Hoeffding, W. (1948) A class of statistics with asymptotically normal distributions. *Ann. Math. Statist.*, **19**,3, pp 293–325
- Kaiser, J. W., Peuch, V.-H., Benedetti, A., Boucher, O., Engelen, R. J., Holzer-Popp, T., Morcrette, J.-J., Wooster, M. J., and the MACC-II Management Board, (2012) The pre-operational GMES Atmospheric Service in MACC-II and its potential usage of Sentinel-3 observations. ESA Special Publication SP-708, Proceedings of the 3rd MERIS/(A)ATSR and OCLI-SLSTR(Sentinel-3) Preparatory Workshop, held in ESA-ESRIN, Frascati, Italy, 15–19 October 2012
- Mayer, B., Kylling, A. (2005) Technical note : The libRadtran software package for radiative transfer calculations – description and examples of use, *Atmos. Chem. Phys.*, **5**, pp 1855–1877
- Peuch, V.-H., Rouil, L., Tarrason, L., and Elbern, H., (2009) Towards European-scale Air Quality operational services for GMES Atmosphere, 9th EMS Annual Meeting. EMS2009-511, 9th European Conference on Applications of Meteorology (ECAM) Abstracts, held 28 September–2 October 2009, Toulouse
- Prigen, C., Aires, F., Rossow, W., Matthews, E. (2001) Joint characterization of vegetation by satellite observations from visible to microwave wavelengths. A sensitivity analysis, *J. Geophys. Res.*, **106**, 20, pp 665-685
- Sobol', I. M. (1993) Sensitivity estimates for nonlinear mathematical models. *Mathematical Modeling & Computational Experiment*, **01**,04, 407–414
- Sobol' I. M., Tarantola S, Gatelli D, Kucherenko SS, Mauntz W., (2007). Estimating the approximation error when fixing unessential factors in global sensitivity analysis. *Reliab. Eng. Syst. Saf.*, **92**, 7, pp 957–960

This copyright notice applies only to the overall collection of papers: authors retain their individual rights and should be contacted directly for permission to use their material separately. Contact EUMETSAT for permission pertaining to the overall volume.

The papers collected in this volume comprise the proceedings of the conference mentioned above. They reflect the authors' opinions and are published as presented, without editing. Their inclusion in this publication does not necessarily constitute endorsement by EUMETSAT or the co-organisers

For more information, please visit [www.eumetsat.int](http://www.eumetsat.int)